# Lack of Content Uniformity in Azacitidine Vials

James T. Isaacs[1], Philip J. Almeter[1, 2], Aaron N. Hunter[1], Thomas A. Lyman[1], Stephanie P. Zapata[1], Bradley S. Henderson[1], Seth A. Larkin[1, 2], Lindsey M. Long[1, 2], Megan N. Bossle[1, 2], Austin M. Lozier[1, 2],Joshua D. Melson[1, 2], Savannah R. Fraley[1, 2], Eunice Hazzel L. Relucio[1, 2], Margaret A. Felix[1], Jeffrey W. Reynolds[3], Ryan W. Naseman[1, 2], Thomas L. Platt[1, 2], Kaylee N Meador[2], Sanda Grahovic[2], Jessica T Rajcan[2], Hyungjoo Shon[2], Anna M Carlson[2], Taylor M Fuson[2], Lian Z Haney[2], Robert A. Lodder[4,*]

University of Kentucky
Lexington, KY

1. Department of Pharmacy Services, University of Kentucky HealthCare, Lexington, KY 40536
2. Pharmacy Practice & Sciences, College of Pharmacy, University of Kentucky, Lexington, KY 40536
3. Department of Finance, University of Kentucky HealthCare, Lexington, KY
4. Department of Pharmaceutical Sciences, University of Kentucky, Lexington, KY 40536

*Author to whom correspondence should be addressed. Email: Lodder @ g.uky.edu
ORCID 0000-0001-6133-7561

## RAPID COMMUNICATION

## Abstract

Azacitidine injections are used to treat specific types of blood cancers. They work by interfering with the growth of cancer cells. Azacitidine for injection is a nucleoside metabolic inhibitor indicated for the treatment of (a) Adult patients with the following FAB myelodysplastic syndrome (MDS) subtypes: Refractory anemia (RA) or refractory anemia with ringed sideroblasts (RARS) (if accompanied by neutropenia or thrombocytopenia or requiring transfusions), refractory anemia with excess blasts (RAEB), refractory anemia with excess blasts in transformation (RAEB-T), and chronic myelomonocytic leukemia (CMMoL), and (b)

Pediatric patients aged 1 month and older with newly diagnosed Juvenile Myelomonocytic Leukemia (JMML).

Intra-lot variability was initially detected in one lot of azacitidine for injection in which 17% of the samples scanned in the lot were more than 5 multidimensional SDs from the center of the lot cluster. After the intra-lot variability was detected, inter-lot variability was measured in a spectral library comprising 8 lots of azacitidine for injection.

# Introduction

The University of Kentucky's (UK) Drug Quality Task Force (DQTF) was established in August of 2019 to engage in consumer-level quality assurance screening for drugs used within UK HealthCare's pharmacies (Isaacs, 2024). The DQTF currently screens medications using Fourier transform near-infrared spectrometry (FTNIR) and Raman spectrometry for potential quality defects indicated by variability in absorbance peak intensities and locations. Through years of continuous monitoring, DQTF has assembled a spectral library containing medications typically used in a health system setting. Statistical analyses using the DQTF spectral library are performed to identify potential intra-lot and inter-lot variability in medications under review. Using Medwatch and publications in the scientific literature, the DQTF reports its findings in an effort to hold manufacturers accountable for GMP requirements and to improve patient outcomes by providing information on quality to augment the information on price that is already available. The increasing transparency is designed to improve the pharmaceutical supply chain.

## Drug Product

Azacitidine for Injection is supplied as a lyophilized powder in 100 mg single-dose vials. Azacitidine for injection is a nucleoside metabolic inhibitor indicated for the treatment of:

1. adult patients with the following FAB myelodysplastic syndrome (MDS) subtypes: Refractory anemia (RA) or refractory anemia with ringed sideroblasts (RARS) (if accompanied by neutropenia or thrombocytopenia or requiring transfusions), refractory anemia with excess blasts (RAEB), refractory anemia with excess blasts in transformation (RAEB-T), and chronic myelomonocytic leukemia (CMMoL)(Dailymed, 2024)(FDA, 2016).
2. Pediatric patients aged 1 month and older with newly diagnosed Juvenile Myelomonocytic Leukemia (JMML)(Dailymed, 2024).

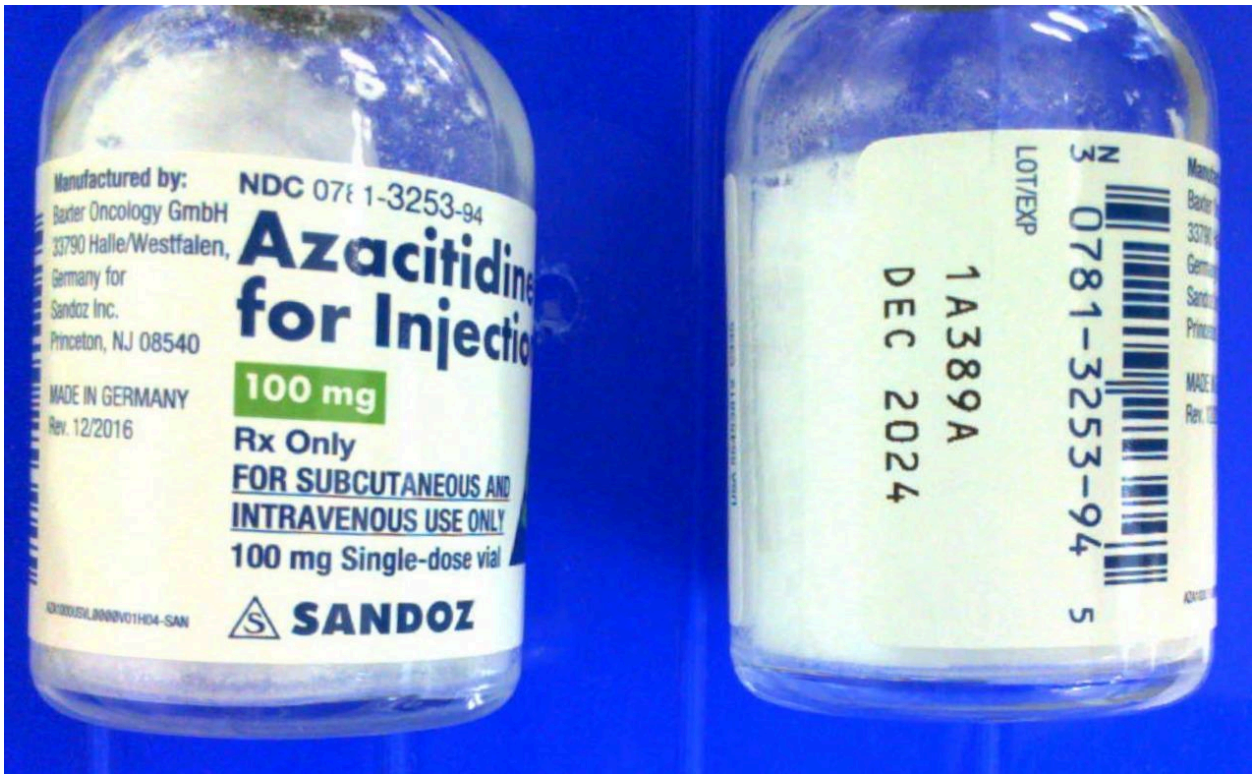


**Figure 1.** Photo of the Azacitidine for Injection drug product from lot 1A389A.

The lot numbers making up the spectral library were 0B273A, 0B276B, 0I349A, 0J355A, 0J363A, 0J367A, 1A389A and 9I232A,. Lots 0J367A and 1A387A were analyzed individually. Figure 1 is a photo of vials from lot 1A389A.

# Background

## Recent studies

A phase Ib study conducted by Sallman et al. (Sallman, 2023) evaluated the safety and efficacy of combining magrolimab, an anti-CD47 monoclonal antibody, with azacitidine in patients with untreated higher-risk myelodysplastic syndromes (MDS). The study included 95 patients, a significant portion of whom had poor-risk cytogenetics and TP53 mutations. The combination therapy demonstrated promising results, with a complete remission (CR) rate of 33% and an overall response rate of 75%. The median progression-free survival was 11.6 months, and the median overall survival was not reached at a 17.1-month follow-up, indicating durable responses. In the subset of patients with TP53 mutations, 40% achieved CR with a median

overall survival of 16.3 months. The treatment was generally well-tolerated, with common adverse effects being constipation, thrombocytopenia, and anemia. These findings support the continued investigation of magrolimab and azacitidine in a phase III trial, highlighting its potential as a new treatment option for higher-risk MDS.

A paper titled "Azacitidine Induced Lung Injury: Report and Contemporary Discussion on Diagnosis and Management" by Alyamany et al. (Alyamany, 2024), addressed the rare but potentially fatal adverse event of lung toxicity caused by azacitidine, a hypomethylating agent used in the treatment of myelodysplastic syndrome (MDS) and acute myeloid leukemia (AML). Azacitidine has significantly improved outcomes for MDS and AML patients not eligible for stem cell transplants. Despite its relatively safe toxicity profile, lung toxicity, though rare, has emerged as a serious complication. The paper delineated the presentation, diagnosis, and management of azacitidine-induced lung injury, supported by a literature review of 20 case reports and the authors' clinical experience.

In the Alyamany paper a 63-year-old male with AML and a history of heavy smoking developed lung toxicity after treatment with azacitidine and venetoclax. Initially, the patient showed improvement after antifungal and antimicrobial treatments, but experienced recurrent severe respiratory symptoms upon resuming azacitidine. Diagnostic challenges included ruling out infections and malignancy. The patient was ultimately diagnosed with azacitidine-induced pneumonitis after comprehensive diagnostic work, including Bronchoalveolar Lavage (BAL) and imaging. Steroid therapy led to clinical improvement, but the patient relapsed and died months later.

Azacitidine inhibits DNA methylation, restoring normal function to tumor suppressor genes. Its adverse effects are generally manageable, but lung toxicity, manifesting as pneumonitis or organizing pneumonia, has been reported in less than 0.1% of cases. Common side effects include cytopenia and gastrointestinal symptoms. Lung toxicity presents with fever, cough, and dyspnea, which can be mistaken for infections. Radiological findings typically show ground-glass opacities and interstitial changes. The exact mechanism is unclear, but proposed theories include:

- Direct Cytotoxicity: Similar to gemcitabine, causing endothelial damage and pulmonary edema.
- Inflammatory and Immune-Mediated Injury: Supported by lymphocytosis in fluid analyses and response to steroids.
- Hypersensitivity Reactions: Both type I and type IV hypersensitivity reactions have been implicated.
- Impaired Repair Mechanisms: Damage to pneumocytes and upregulation of collagen synthesis leading to fibrosis.

Potential risk factors include a history of smoking, previous lung infections, and existing pulmonary conditions. Differential diagnoses include infections, malignancy, autoimmune diseases, and drug-induced lung injuries from other medications. Diagnosis is primarily clinical and relies on ruling out other causes. Key steps include:

- Detailed history and physical examination.
- Extensive microbiological investigations.
- Imaging studies, especially CT scans.
- Pathological examination, if feasible.

The mainstay of treatment is discontinuation of azacitidine and initiation of corticosteroids. The response to treatment is typically favorable if initiated early. In some cases, azacitidine can be replaced with decitabine, although close monitoring is necessary. Azacitidine-induced lung injury, while rare, requires prompt recognition and management to prevent severe outcomes. Further research is needed to better understand the mechanisms and optimize treatment protocols. The paper provides an algorithm to aid clinicians in diagnosing and managing this condition effectively.

## Shortages

Azacitidine Injection is listed as Currently in Shortage (FDA Drug Shortages, 2024). The date the shortage was first posted was 12/18/2020. The Sandoz product is not currently on the shortage list. But under the shortage, firms like Intas Pharmaceuticals Limited whose products have been refused admission into the US due to lack of CGMP compliance are permitted by FDA to ship azacitidine for injection into the US on a batch-by-batch basis (FDA, 2023), subject to certain conditions:

Independent Third-Party Oversight:

- Batch Certification: An independent third party must certify each batch's quality, ensuring it meets standards and has no data integrity issues or unresolved out-of-specification (OOS) events.
- Comprehensive Investigations: Any OOS or unexpected result triggers a thorough investigation, documented and approved by the third party, with special attention to test results.
- Proactive FDA Notification: The FDA must be notified before releasing any batch associated with an OOS, regardless of eventual certification.
- Detailed Record Evaluation: The third party reviews all batch manufacturing records, test results (including electronic data), deviations, OOS events, environmental monitoring, and visual inspection records.

- Timely Certification: Retrospective batch certification occurs within 45 days of release or distribution and is submitted to the FDA.
- Rapid Alert for Concerns: If the third party has significant concerns about a released batch, the FDA is notified within 3 working days via a Field Alert Report (FAR) and directly to the Drug Shortage Staff (DSS) for further discussion on appropriate subsequent actions..

. Additional Testing and Information:

- Triplicate Testing: Batches already manufactured, on hold, or pending distribution undergo triplicate testing by an independent lab.
- Certificate of Analysis (COA) Provision: Both original and triplicate testing COAs are provided to the FDA.
- Independent Lab Details: The FDA receives information about the chosen independent lab, including qualifications, method verification, and a list of batches to be tested.
- Sample Retention: Sufficient samples from on-hold batches are retained for potential FDA testing.
- Immediate Issue Reporting: The DSS is immediately informed of sterility or stability failures, complaints, and OOS results, with a FAR filed if necessary.
- Stability Data Provision: Stability data supporting referenced batches is provided upon request, with additional batches added to stability studies as needed.
- Comprehensive Protocol: A detailed protocol outlining the scope, impartiality controls, third-party qualifications, review timelines, and expected outcomes is provided.

### FDA Medwatch

An FDA Form 3500 Medwatch describing the findings of this Rapid Communication was filed.

# Methods

## FTNIR (Fourier Transform Near-Infrared) Spectrometry

Using nondestructive analytical techniques, FTNIR spectra were collected from inventory as part of routine medication quality screening. A representative sample of individual vials were selected for screening and noted to be stored under the conditions required by the manufacturer in their original packaging. FTNIR spectra were collected noninvasively and nondestructively through the bottom of the vials using a Thermo Scientific Antaris II FTNIR Analyzer (Waltham, MA, USA)(Isaacs, 2023a).

## Smoothing

Data smoothing is a technique used to remove noise from data. This can be done by fitting a smooth curve to the data, such as a cubic spline. Cubic splines are piecewise cubic polynomials that are continuous and have continuous first and second derivatives. This makes them very smooth and resistant to noise. Cubic splines can be easily fitted to data using least squares (Matlab, 2023)(Pollock, 1998).

## Multiplicative Scatter Correction (MSC)

Multiplicative scatter correction (MSC) is a widely used spectrometric normalization technique. Its purpose is to correct spectra in such a way that they are as close as possible to a reference spectrum, generally the mean of the data set, by changing the scale and the offset of the spectra (Isaksson, 1988).

## BEST (Bootstrap Error-Adjusted Single-sample Technique)

The BEST calculates distances in multidimensional, asymmetric, nonparametric central 68% confidence intervals in spectral hyperspace (roughly equivalent to standard deviations)(Dempsey, 1996). The BEST metric can be thought of as a "rubber yardstick" with a nail at the center (the mean). The stretch of the yardstick in one direction is therefore independent of the stretch in the other direction. This independence enables the BEST metric to describe odd shapes in spectral hyperspace (spectral point clusters that are not multivariate normal, such as the calibration spectra of many biological systems). BEST distances can be correlated to sample composition to produce a quantitative calibration, or simply used to identify similar regions in a spectral image. The BEST automatically detects samples and situations unlike any encountered in the original calibration, making it more accurate in chemical investigation than typical regression approaches to near-IR analysis. The BEST produces accurate distances even when the number of calibration samples is less than the number of wavelengths used in calibration, in contrast to other metrics that require matrix factorization. The BEST is much faster to calculate as well (O(n) instead of the $O(n^3)$ required by matrix factorization.

## Principal Components (PCs)

Principal component analysis is the process of computing the principal components of a dataset and using them to execute a change of basis (change of coordinate system) on the data, usually employing only the first few principal components and disregarding the rest (Joliffe, 2016). PCA is used in exploratory data analysis and in constructing predictive models. PCA is commonly utilized for dimensionality reduction by projecting each data point onto only the first few principal components to obtain lower-dimensional data while preserving as much of the original variation in the data as possible. The first principal component is the direction that maximizes the variance of the projected data. The second principal component is the direction of the largest variance orthogonal to the first principal component. Decomposition of the variance typically

continues orthogonally in this manner until some residual variance criterion is met. Plots of PC scores help reveal underlying structure in data.

## Subcluster Detection

In typical near-infrared multivariate statistical analyses, samples with similar spectra produce points that cluster in a certain region of spectral hyperspace. These dusters can vary significantly in shape and size due to variation in sample packings, particle-size distributions, component concentrations, and drift with time. These factors, when combined with discriminant analysis using simple distance metrics, produce a test in which a result that places a particular point inside a particular cluster does not necessarily mean that the point is actually a member of the cluster. Instead, the point may be a member of a new, slightly different cluster that overlaps the first. A new cluster can be created by factors like low-level contamination, moisture uptake, or instrumental drift. An extension added to part of the BEST, called FSOB (Fast Son of BEST) can be used to set nonparametric probability-density contours inside spectral clusters as well as outside (Isaacs, 2023b)(Lodder, 1988), and when multiple points begin to appear in a certain region of cluster-hyperspace the perturbation of these density contours can be detected at an assigned significance level using r values, and visualized using quantile-quantile (QQ) plots. The detection of unusual samples both within and beyond 3 SDs of the center of the training set is possible with this method. Within the ordinary 3 SD limit, however, multiple instances are needed to detect unusual samples with statistical significance.

## Artificial Intelligence Tools

Artificial intelligence (AI) tools, principally used for background information, include Gemini (Google LLC) and GPT-4 (OpenAI). AI can be used in a variety of ways, including to brainstorm, organize thoughts, develop arguments, and edit.

# Results and Discussion

## Intralot analysis

### Spectra

Smoothed spectral graphs of the 6 vials sampled from lot 0J367A are shown in Figure 2 and Figure 3. Two spectral regions show the difference between the outlier vial (vial number 3, depicted with a gold line) and the remaining vials. These two differentiating spectral regions are 4100 to 4800 and 5700 to 5950 $cm^{-1}$. Vial 3 has a more intense peak at about 4625 $cm^{-1}$ than the other vials from the same lot, and vial 3 is missing peaks at about 4220 and 4280 cm-1 that

the other vials show. Furthermore, vial 3 exhibits more pronounced peaks at approximately 5910, 5795, and 5750 $cm^{-1}$ compared to the other vials in lot 0J367A.

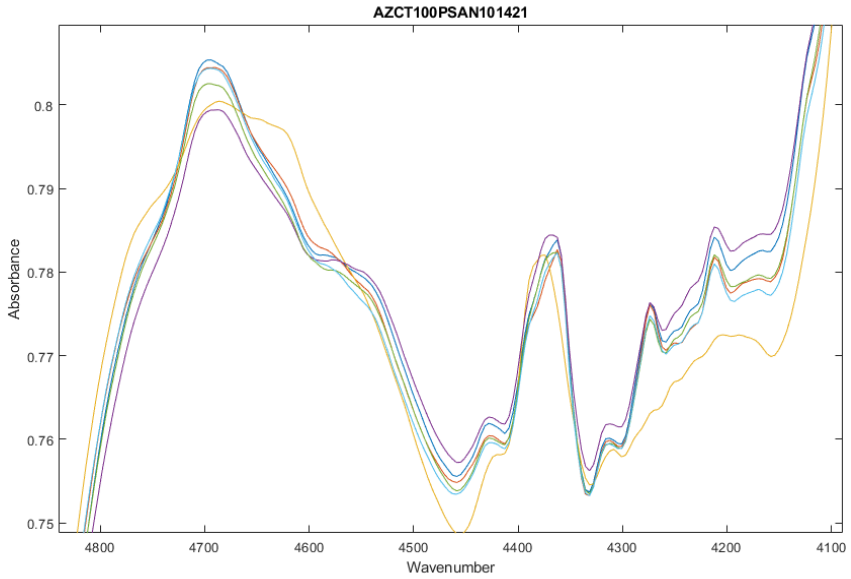


**Figure 2**. Spectra of vials in lot 0J367A. Vial 3 (gold) in the set appears 5.4 SDs from the other vials in the lot. Vial 3 has a stronger peak at about 4625 $cm^{-1}$ than the other vials from the same lot, and is missing peaks at about 4220 and 4280 $cm^{-1}$ that the other vials possess.

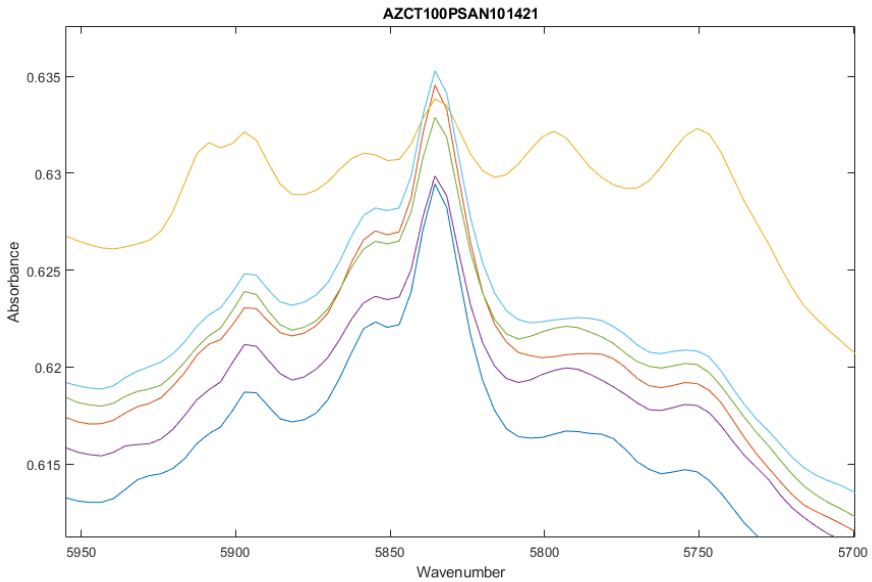


**Figure 3**. Spectra of vials in lot 0J367A. Vial 3 (gold) in the set appears 5.4 SDs from the other vials in the lot. Vial 3 has stronger peaks at about 5910, 5795, and 5750 $cm^{-1}$ than the rest of the set of vials from lot 0J367A.

## PC Plot

A plot of the principal component scores of the spectra of the vials in Figure 2 and Figure 3 is shown in Figure 4. Vial 3 from Figure 2 and Figure 3 appears at the far right of the plot. When a principal component score of a spectral data point is displaced from the rest of the cluster, it indicates that the data point is an outlier or has unique characteristics compared to the rest of the spectral data points in that cluster. This is useful in identifying special cases or anomalies within the spectral dataset.

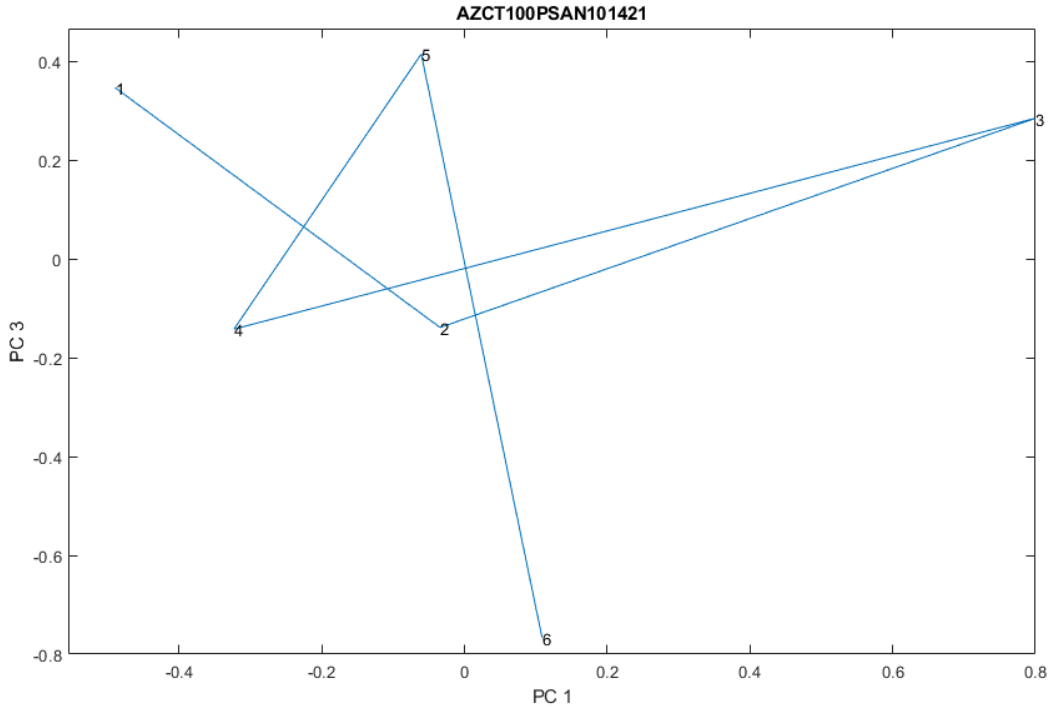


**Figure 4.** Principal component scores of the spectra of the samples from lot 0J367A. Vial 3 from Figure 2 and Figure 3 appears at the far right of the plot. Vial 3 is 5.4 multidimensional SDs from the other vials from the lot.

## Interlot analysis

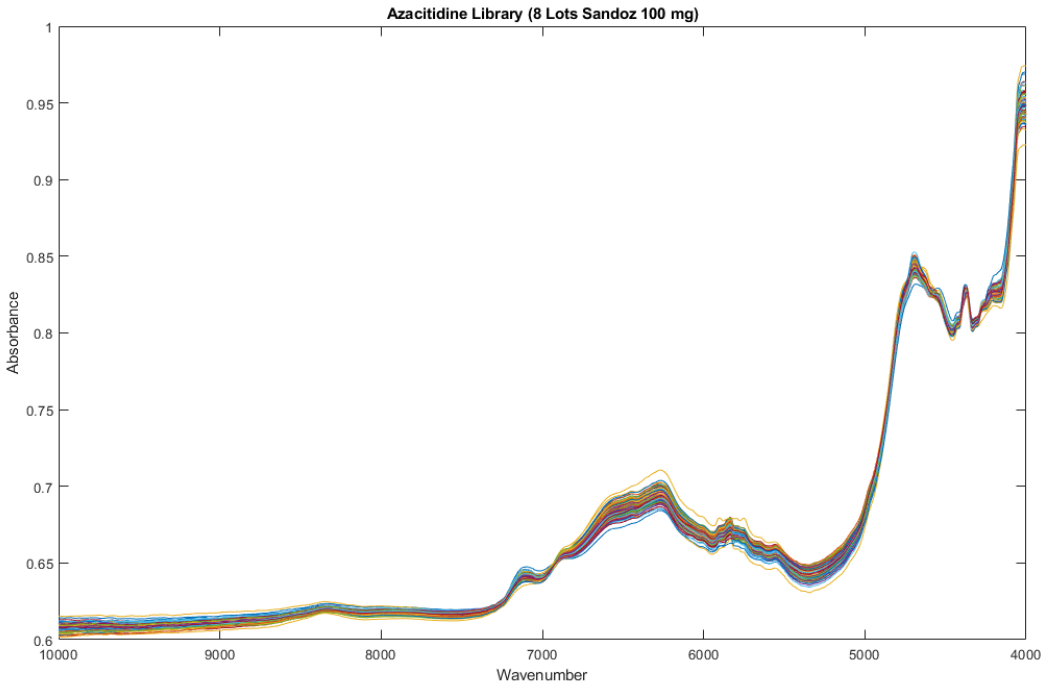


**Figure 5.** Full spectra of the library of 84 vials from 8 lots of azacitidine.

The full near-infrared spectra of 84 vials from 8 lots of azacitidine in the spectral library appear in Figure 5. For a difference in the spectra to show up in this type of graph the difference would typically have to be on the first or second principal component, which are the largest two sources of spectral variation by definition.

### PC Plots

Principal component scatterplots of the spectra of the entire library of 84 vials appear in Figure 6, Figure 7, and Figure 8. Figure 6 is a scatterplot of the spectral data of the library using PCs 1, 2, and 3. No vials appear to be outliers in Figure 6 on inspection or when measured in BEST SDs. Figure 7 is a scatterplot of the spectral data of the library on PCs 4, 5, and 6. Now one vial appears to be an outlier, vial number 45. Vial 45 measures 7.3 multidimensional SDs from the center of the spectral library cluster on PCs 4, 5, and 6. Four additional vials are between 3 and 4 SDs from the center on PCs 4, 5, and 6. Figure 8 is a scatterplot of the vials in the library on PCs 7, 8, and 9. Four vials In the spectral library plot more than three SDs from the center on PCs 7, 8, and 9. Vial 28 is 5.3 SDS away from the center, vial 57 is 3.2 SDs away, vial 59 is 4.5 SDs away, and vial 77 is 3.3 SDs away.

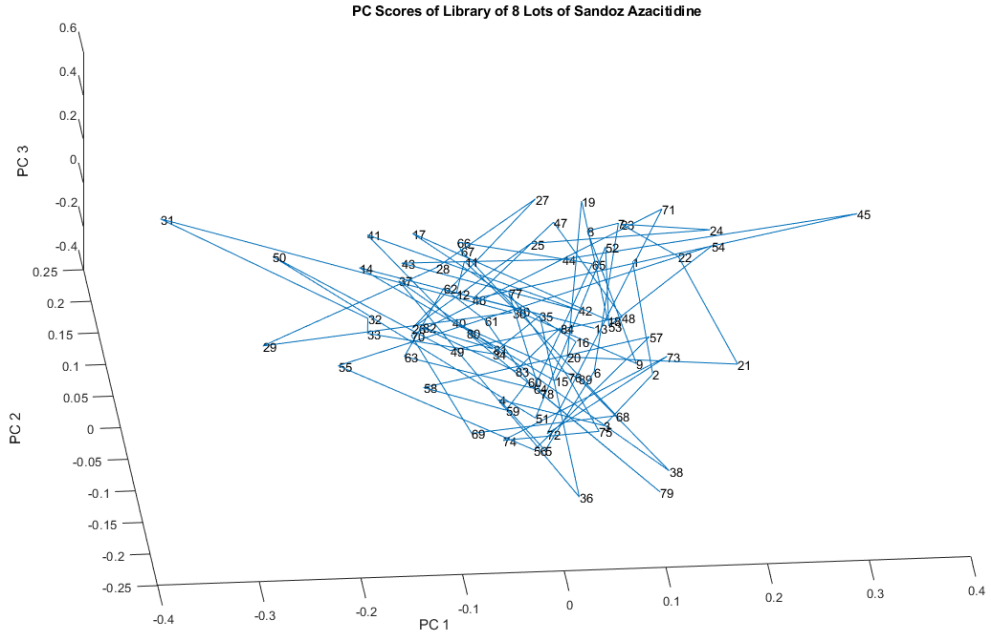


**Figure 6.** A scatterplot of the spectral data of the library using PCs 1, 2, and 3.

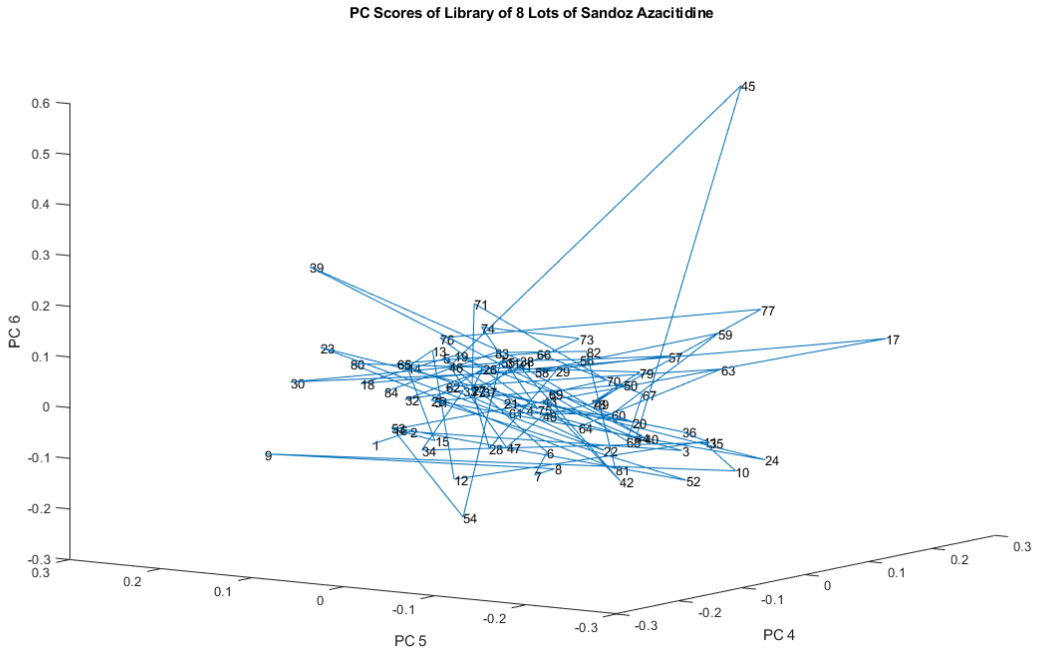


**Figure 7.** A scatterplot of the spectral data of the library on PCs 4, 5, and 6. One vial appears to be a possible outlier, vial number 45. Vial 45 measures 7.3 multidimensional SDs from the center of the spectral library cluster.

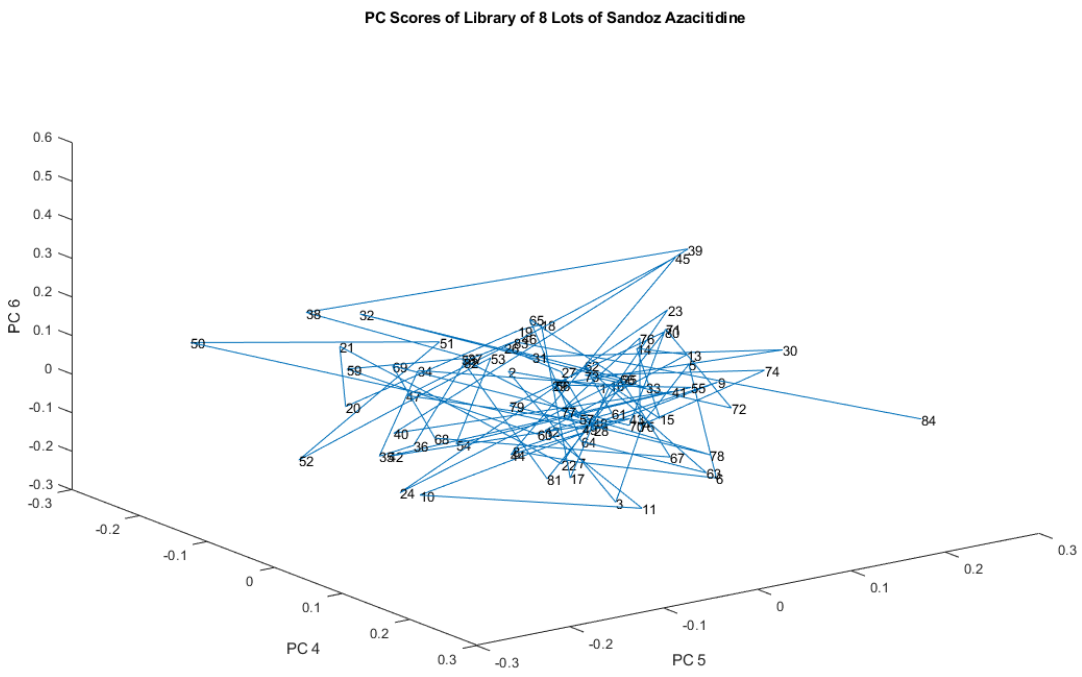


**Figure 8.** A scatterplot of the vials in the library on PCs 7, 8, and 9.

## QBEST Results

Full spectral measurements of BEST distances in SDs reveal two outliers in the library, vial 31 and vial 45. Vial 31 is 3.6 multi-dimensional SDs from the center of the cluster of the library. Vial 45 is also 3.6 SDs away from the center of the library cluster.

Table 2 shows the variation accounted for by each of the principal components of the spectra in the library. If a library of pharmaceuticals is very homogeneous, PC 1 will contain 90% or more of the total spectral variation. As more outliers creep into the data, more variation appears on lower PCs. Almost 25% of the total spectral variation is on PC number 2 for the spectral library, suggesting a possible problem with production.

**Table 2:** Variation accounted for by each of the principal components of the spectra in the library

| PC Number | Variation in this PC | Cumulative PC Variation |
|---|---|---|
| **1** | 0.6660 | 0.6660 |
| **2** | 0.2453 | 0.9113 |
| **3** | 0.0328 | 0.9441 |

| | | |
|---|---|---|
| **4** | 0.0163 | 0.9605 |
| **5** | 0.0152 | 0.9757 |
| **6** | 0.0090 | 0.9846 |
| **7** | 0.0070 | 0.9916 |
| **8** | 0.0035 | 0.9951 |
| **9** | 0.0011 | 0.9962 |

## PC Loadings Plots

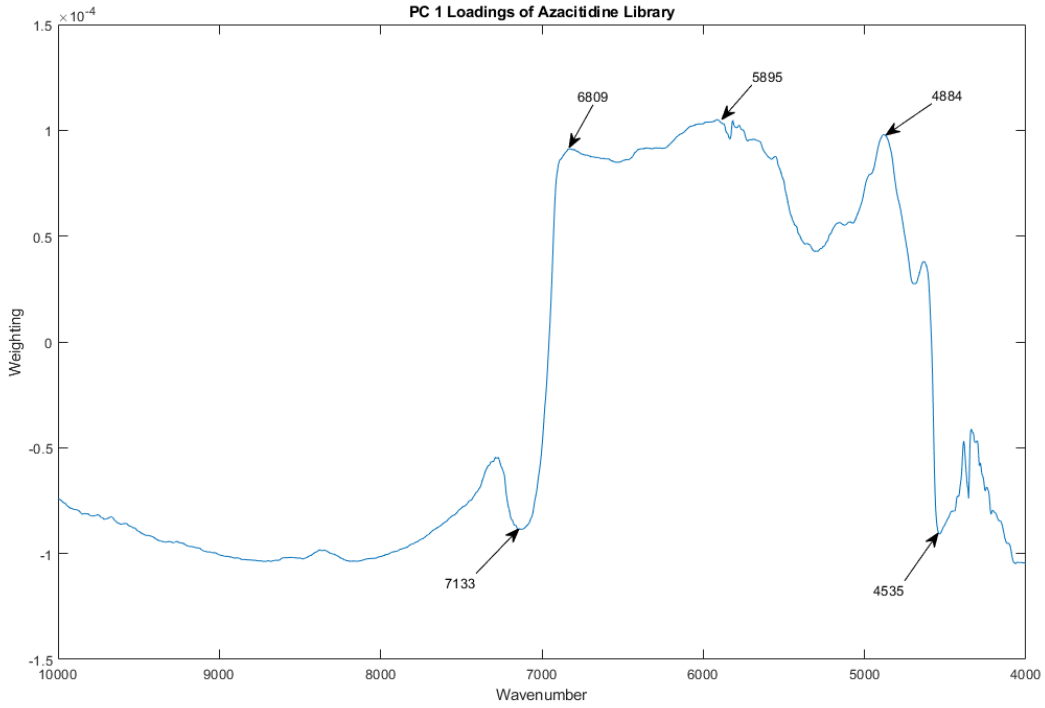


**Figure 9.** A plot of the principal component loadings for PC 1 of the azacitidine library. PC 1, as is typical in drugs, shows the effects of baseline variation after multiplicative scatter correction.

Figure 9 is a graph of the loadings that form principal component 1. The PC 1 loadings primarily show the effect of multiplicative scatter correction. Important peaks at 4535, 4884, 5895, 6609, and 7133 $cm^{-1}$ are marked with arrows. Figure 10 is a plot of the loadings of the spectral library for PC 2. The loadings begin to reflect the chemical composition of the drug more by the second component. The main peaks at 4308, 4664, 5299, 6543, and 7282 $cm^{-1}$ are marked with arrows.

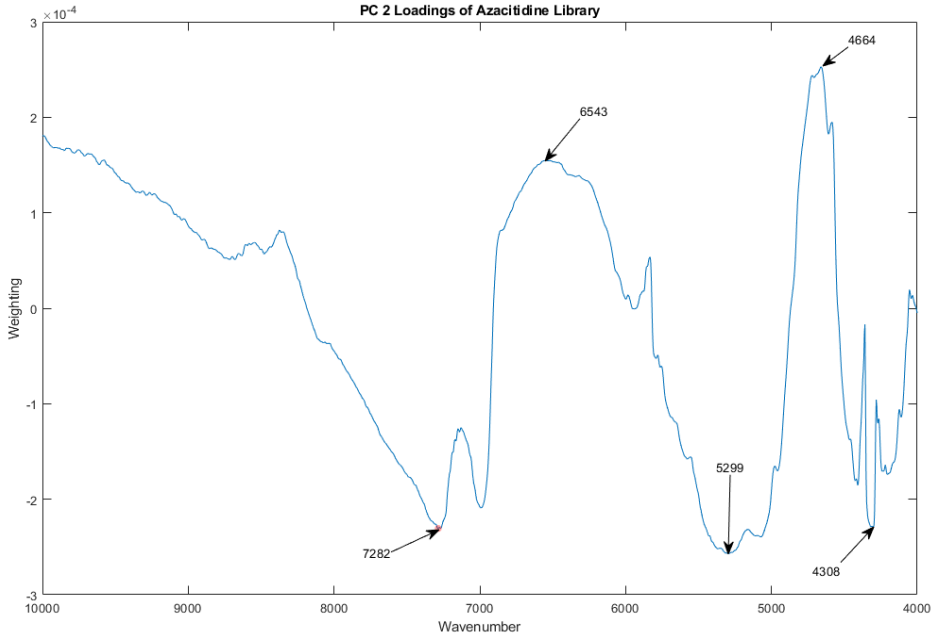


**Figure 10.** A plot of the loadings of the spectral library for PC 2.

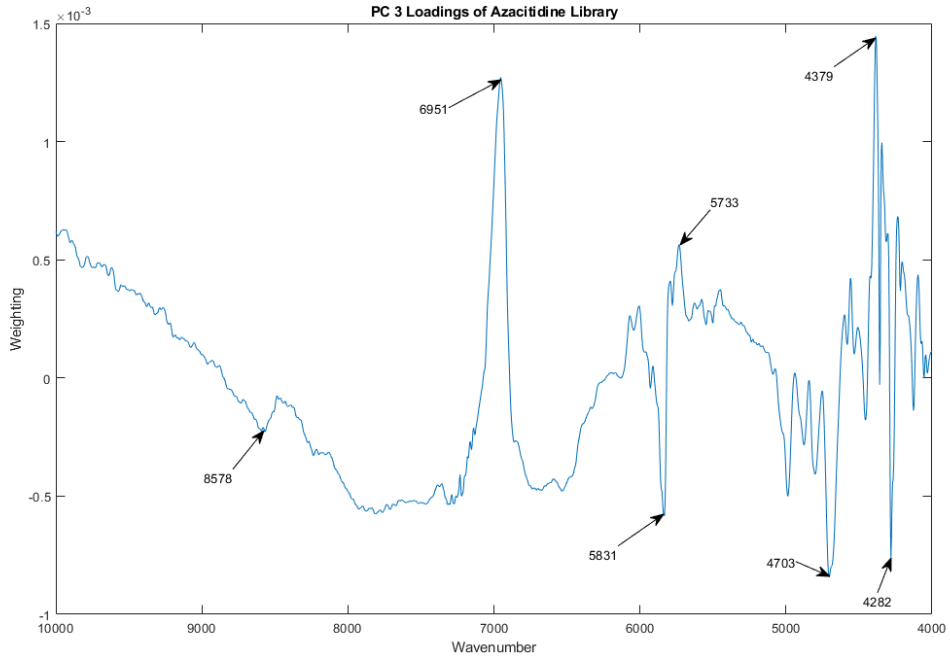


**Figure 11.** A plot of the loadings of the spectral library for PC 3.

Figure 11 is a plot of the loadings of the spectral library for PC 3. The main peaks at 4282, 4379, 4703, 5733, 5831, 6951, and 8578 $cm^{-1}$ are marked with arrows. In Figure 11 it looks like there is more noise in the low wavenumber region of the spectra shown on the right than In the high wavenumber region on the left. However, this is actually the least noisy area in the spectrum and all of these peaks represent chemical features of the vials.

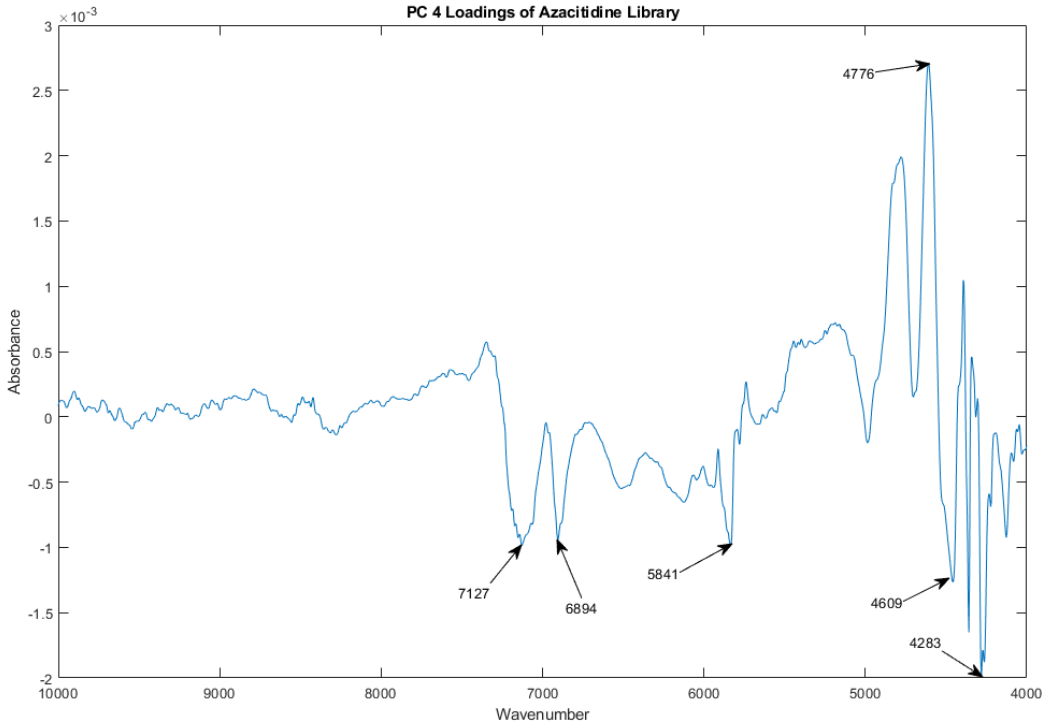


**Figure 12.** A plot of the loadings of the spectral library for PC 4.

Figure 12 is a plot of the loadings of the spectral library for PC 4. Dominant spectral peaks at 4283, 4609, 4776, 5841, 6894, and 7127 $cm^{-1}$ are denoted with arrows. Figure 13 is a plot of the loadings of the spectral library for PC 5.

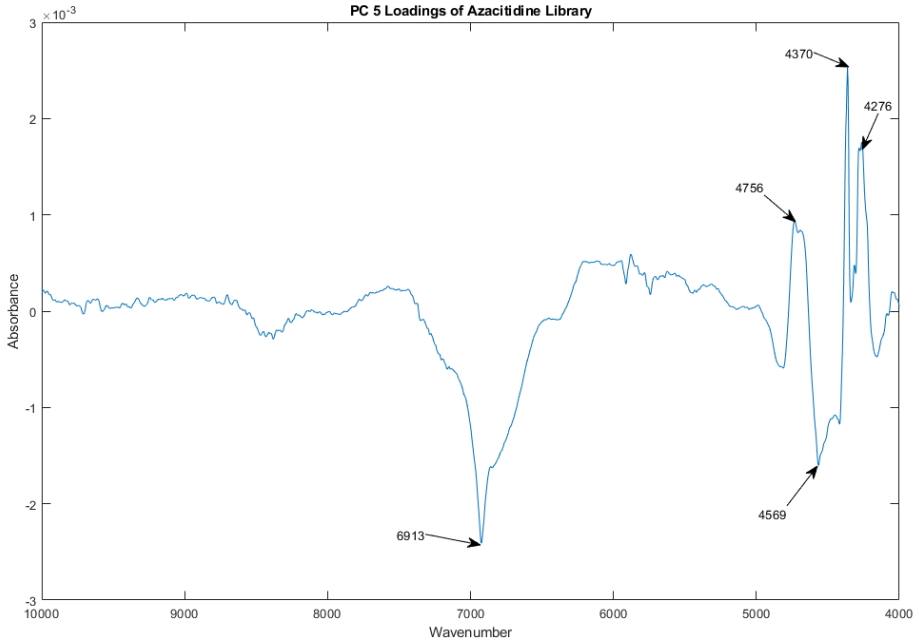


**Figure 13.** A plot of the loadings of the spectral library for PC 5

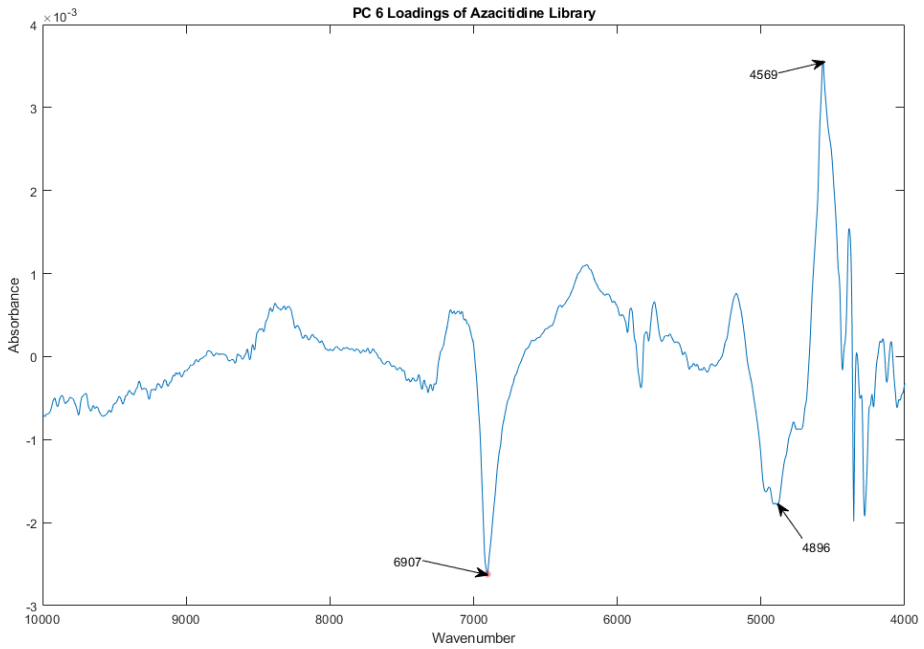


**Figure 14.** A plot of the loadings of the spectral library for PC 6.

Figure 14 is a plot of the loadings of the spectral library for PC 6. Noise is beginning to creep into the loadings from the high-wavenumber end of the spectrum. The chief peaks at 4569, 4896, and 6907 $cm^{-1}$ are marked with arrows.

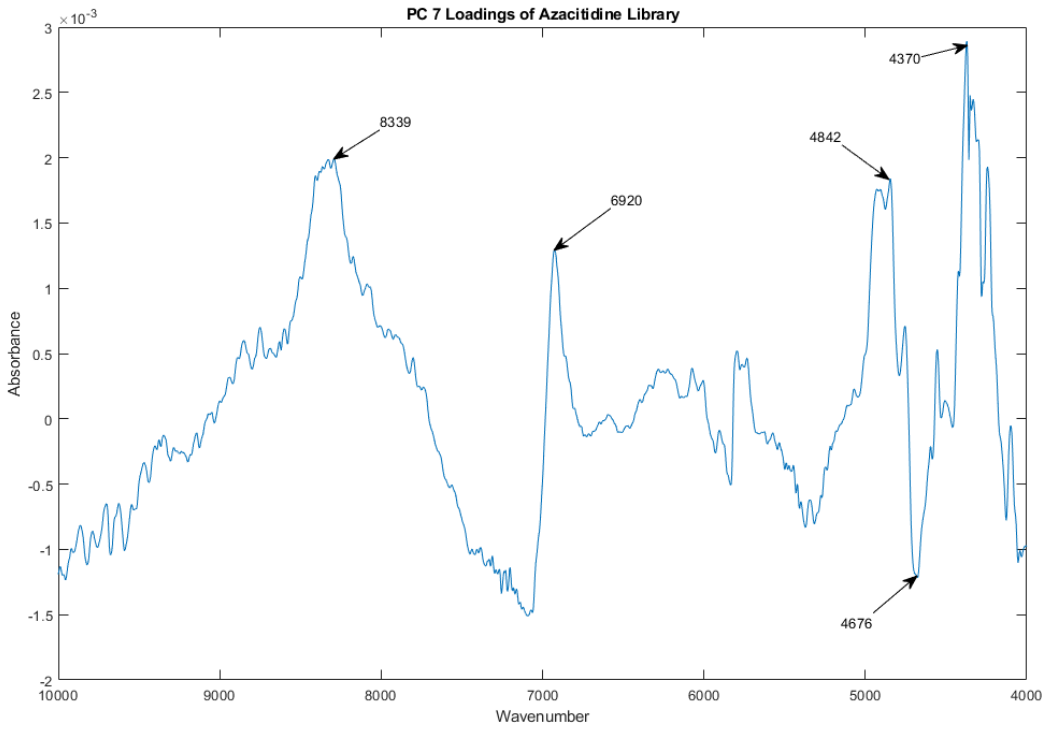


**Figure 15.** A plot of the loadings of the spectral library for PC 7

Figure 15 is a plot of the loadings of the spectral library for PC 7. The major peaks at 4370, 4676, 4842, 6920, and 8339 $cm^{-1}$ are marked with arrows. Figure 16 is a plot of the loadings of the spectral library for PC 8. The main peaks at 4270, 4749, 4969, 5841, and 6933 $cm^{-1}$ are marked with arrows. Figure 17 is a plot of the loadings of the spectral library for PC 9. By PC 9 noise has moved in from the high-wavenumber end of the spectrum. The predominant peaks at 4330, 4356, 6920, and 7220 are pointed out with arrows.

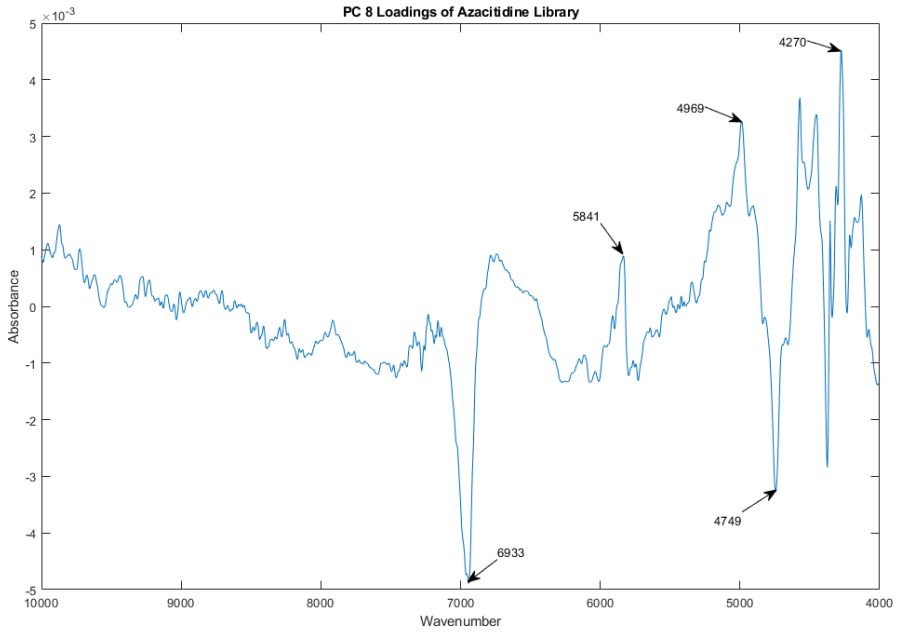


**Figure 16**. A plot of the loadings of the spectral library for PC 8.

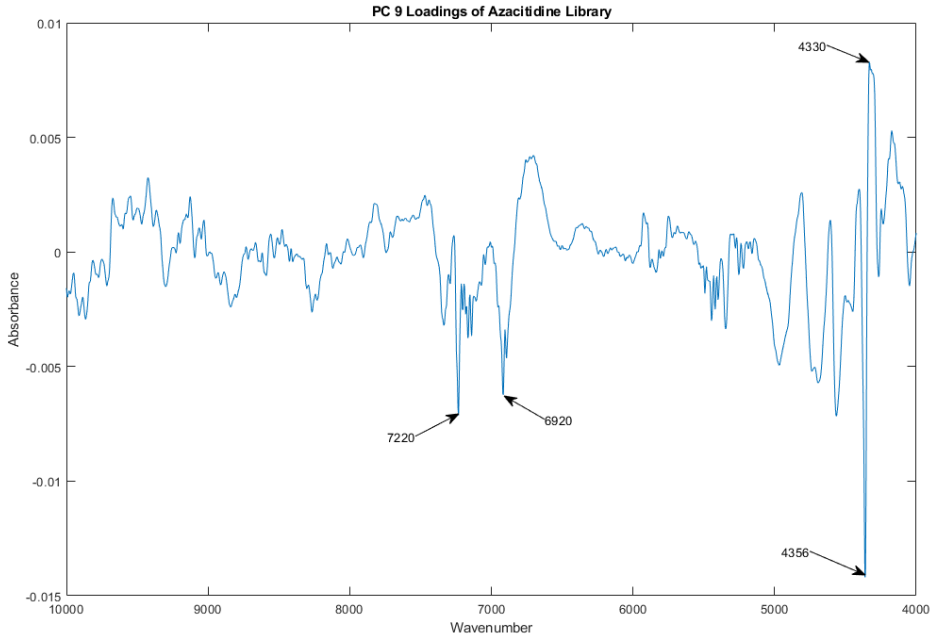


**Figure 17.** A plot of the loadings of the spectral library for PC 9.

# Conclusion

This study explored the variability in the content of azacitidine vials, a drug used for treating specific blood cancers. The University of Kentucky's Drug Quality Task Force (DQTF) identified significant intra-lot and inter-lot variability in azacitidine vials through the use of Fourier transform near-infrared spectrometry (FTNIR). These variations suggest potential issues in the manufacturing process, which may not adhere to GMP. The study highlights the importance of consumer-level quality assurance screening to ensure drug safety and efficacy, and the findings were reported to the US FDA in an effort to improve the pharmaceutical supply chain.

Intralot variability was detected first in one lot of the drug. This detection prompted additional investigation of the eight lots previously scanned that form the spectral library for azacitidine.for investigation of interlot variability. These spectrometric results do not prove an excess level of impurities or adulteration. However, they suggest that the manufacturing process may have been operating outside of a state of process control. Additional investigation is needed.

## Acknowledgements

The project described was supported in part by the National Center for Research Resources and the National Center for Advancing Translational Sciences, National Institutes of Health, through Grant UL1TR001998. The content is solely the responsibility of the authors and does not necessarily represent the official views of the NIH.

## References

Alyamany, R., Alnughmush, A., Almutlaq, M., Alyamany, M., & Alfayez, M. (2024). Azacitidine induced lung injury: report and contemporary discussion on diagnosis and management. Frontiers in Oncology, 14, 1345492.

Dailymed (2024), AZACITIDINE- azacitidine injection, powder, lyophilized, for solution, Sandoz Inc., https://dailymed.nlm.nih.gov/dailymed/fda/fdaDrugXsl.cfm?setid=87f7a39d-06db-48ca-be21-9e8806608439&type=display, retrieved Aug 11 2024

Dempsey, R. J., Davis, D. G., Buice Jr, R. G., & Lodder, R. A. (1996). Biological and medical applications of near-infrared spectrometry. Applied Spectroscopy, 50(2), 18A-34A.

FDA (2016) Highlights Of Prescribing Information, Azacitidine For Injection, https://www.accessdata.fda.gov/drugsatfda_docs/label/2016/208216s000lbl.pdf, retrieved Jun. 12, 2024.

FDA (2023), https://www.fda.gov/media/169115/download, retrieved Jun 15, 2024.

FDA Drug Shortages, (2024) https://www.accessdata.fda.gov/scripts/drugshortages/dsp_ActiveIngredientDetails.cfm?AI=Azacitidine+Injection&st=c&tab=tabs-4&panels=1, retrieved May 13, 2024

Isaacs, J.T., Almeter, P.J., Hunter, A.N., Lyman, T.A., Zapata, S.P., Henderson, B.S., Larkin, S.A., Long, L.M., Bossle, M.N., Bhaktawara, S.A. and Warren, M.F., (2024). Application of Near-Infrared Spectroscopy for Screening of Chlorothiazide Sodium Vials, Contact in context, 1-26. DOI: 10.6084/m9.figshare.25773429

Isaacs, J.T., Almeter, P.J., Hunter, A.N., Lyman, T.A., Zapata, S.P., Henderson, B.S., Larkin, S.A., Long, L.M., Bossle, M.N., Bhaktawara, S.A. and Warren, M.F., (2023a). Assessment of Vecuronium Quality Using Near-Infrared Spectrometry. Contact in context, 1-27. DOI: 10.6084/m9.figshare.24846285

Isaacs, J.T., Almeter, P.J., Henderson, B.S., Hunter, A.N., Platt, T.L., & Lodder, R.A. Nonparametric Subcluster Detection in Large Hyperspaces, (2023b) CIC Computational Sciences, 1-24. DOI:10.6084/m9.figshare.23877213

Isaksson, T., & Næs, T. (1988). The effect of multiplicative scatter correction (MSC) and linearity improvement in NIR spectroscopy. Applied Spectroscopy, 42(7), 1273-1284. https://doi.org/10.1366/0003702884429869

Jolliffe, I. T., & Cadima, J. (2016). Principal component analysis: a review and recent developments. Philosophical Transactions of the Royal Society A: Mathematical, Physical and Engineering Sciences, 374(2065), 20150202.

Lodder, R. A., & Hieftje, G. M. (1988). Detection of subpopulations in near-infrared reflectance analysis. Applied spectroscopy, 42(8), 1500-1512.

Matlab. Smoothing Splines. https://www.mathworks.com/help/curvefit/smoothing-splines.html. Retrieved May 28, 2023.

Pollock, D. S. G. (1993). Smoothing with cubic splines. https://www.physics.muni.cz/~jancely/NM/Texty/Numerika/CubicSmoothingSpline.pdf. Retrieved May 28, 2023.

Sallman, D. A., Al Malki, M. M., Asch, A. S., Wang, E. S., Jurcic, J. G., Bradley, T. J., ... & Daver, N. G. (2023). Magrolimab in combination with azacitidine in patients with higher-risk myelodysplastic syndromes: final results of a phase Ib study. Journal of Clinical Oncology, 41(15), 2815-2826.